Abrogation of Prostaglandin E_2/EP4 Signaling Impairs the Development of *rag1*$^+$ Lymphoid Precursors in the Thymus of Zebrafish Embryos[1]

Eduardo J. Villablanca,*† Anna Pistocchi,‡ Felipe A. Court,§ Franco Cotelli,‡ Claudio Bordignon,* Miguel L. Allende,¶ Catia Traversari,‖ and Vincenzo Russo[2]*

PGE_2 is involved in a wide variety of physiological and pathological processes; however, deciphering its role in early mammalian development has been difficult due to the maternal contribution of PGE_2. To overcome this limitation we have investigated the role of PGE_2 during T cell development in zebrafish. In this study, we show that zebrafish *ep4a*, a PGE_2 receptor isoform of EP4, is expressed at 26 h postfertilization in the dorsal aorta-posterior cardinal vein joint region, which has a high homology with the mammal aorta-gonad-mesonephros area and where definitive hemopoiesis arises. Furthermore, it is expressed in the presumptive thymus rudiment by 48 h postfertilization. Supplementation of PGE_2 results in a strong increase in *rag1* levels and cell proliferation in the thymus. In contrast, the inhibition of PGE_2 production, as well as EP4 blockade, abrogates the expression of *rag1* in the thymus and that of the lymphoid precursor marker *ikaros*, not only in the dorsal aorta-posterior cardinal vein joint region but also in the newly identified caudal hemopoietic tissue without affecting early hemopoietic (*scl*, *gata2*) and erythropoietic (*gata1*) markers. These results identify *ep4a* as the earliest thymus marker and define a novel role for the PGE_2/EP4 pathway in controlling T cell precursor development in zebrafish. ***The Journal of Immunology,*** **2007, 179: 357–364.**

Prostaglandins are lipid-derived autocoids produced by membrane arachidonic acid by virtue of the sequential activity of cyclooxygenase (COX)[3] 1, COX2, and PG synthases (1, 2). PGE_2 is one of the major COX products, inducing a plethora of effects under a number of physiological conditions. PGE_2 regulates diverse functions of many cell types of the immune system, including dendritic cells, macrophages, and T and B lymphocytes (1, 3, 4). However, in T cells as well as in thymus development little is known about the contribution of PGE_2. PG biosynthetic enzymes and receptors have been detected in human, mouse, and rat thymi (5, 6). Thymic cell lines secrete prostaglandins by virtue of the activity of COX1 and COX2 enzymes (7). Moreover, it has been reported that COX1 plays a key role in the transition of immature $CD4^-CD8^-$ double-negative (DN) thymocytes to $CD4^+CD8^+$ double-positive (DP) thymocytes (7). Additionally, COX2 is involved in the formation of CD4 single-positive thymocyte subsets and in their subsequent adherence to medullary stromal cell lines (7). COX2 inhibitors (COX2-inh) can also affect T cell development in a COX2- and PGE_2-independent manner (8).

In mammals, four different PGE_2 G-coupled protein receptors have been identified to date, which gives rise to the functional specificity of PGE_2 in different tissues (1). In vitro experiments have elucidated the role of the EP2 receptor in protecting the Tsup-1 $CD4^+CD8^+$ thymocyte cell line from apoptosis (9) and during the DN to DP transition (7). A role for the EP1 receptor in supporting early thymocyte proliferation and differentiation has also been described (7). There are no reports indicating a role for EP3 or EP4 in thymus development.

The role of PGE_2 in early mammalian T cell development in vivo is unknown and has been refractory to analysis due to the maternal contribution of PGE_2 from the uterus. The zebrafish has become a powerful vertebrate model, offering several advantages over other models for studying both the role of prostaglandins and thymus/T cell development (10–14). Eggs are externally fertilized and therefore cannot be influenced by the contribution of PGs from the uterus. Furthermore, the early steps of lymphopoiesis in zebrafish are similar to those in mammals. T cell maturation takes place in the thymus as it does in mice and humans. The thymus rudiment can be detected at 72 h postfertilization (hpf) by the expression of the thymic epithelium marker *foxn1* (15) and the lymphoid precursor marker *ikaros* (16). Thymus development, especially during the initial stages, requires colonization from hemopoietic sites by the migration of T cell precursors (17). In zebrafish, as in mammals, hemopoiesis is divided in two waves (18); these are primitive hemopoiesis, which predominantly

*Cancer Gene Therapy Unit, Cancer Immunotherapy and Gene Therapy Program, Scientific Institute H. San Raffaele, Milan, Italy; †International Ph.D. Program in Molecular Medicine, University "Vita-Salute" S.Raffaele, Milan, Italy; ‡Department of Biology, University of Milan, Milan, Italy; §Departamento de Ciencias Fisiológicas, Facultad de Ciencias Biológicas, Universidad Católica, Santiago, Chile; ¶Millennium Nucleus in Developmental Biology, Facultad de Ciencias, Universidad de Chile, Santiago, Chile; and ‖MolMed SpA, Milan, Italy

Received for publication January 26, 2007. Accepted for publication April 17, 2007.

The costs of publication of this article were defrayed in part by the payment of page charges. This article must therefore be hereby marked *advertisement* in accordance with 18 U.S.C. Section 1734 solely to indicate this fact.

[1] This work was supported by a grant from Fondazione Cariplo. M.L.A. was supported by grants from Fondo Nacional de Desarrollo Científico y Tecnológico (1031003), Iniciativa Científica Milenio (P02-050), and International Center for Genetic Engineering and Biotechnology (CRP/CHI03-03c).

[2] Address correspondence and reprint requests to Dr. Vincenzo Russo, Cancer Gene Therapy Unit, Scientific Institute S. Raffaele, Via Olgettina 58 Milan, Italy. E-mail address: v.russo@hsr.it

[3] Abbreviations used in this paper: COX, cyclooxygenase; AGM, aorta-gonad-mesonephros; CHT, caudal hemopoietic tissue; DA-PCV, dorsal aorta-posterior cardinal vein; DN, double negative; DP, double positive; dpf, days postfertilization; hpf, hours postfertilization; HSC, hemopoietic stem cell; ICM, intermediate cell mass; inh, inhibitor; MO, morpholino oligonucleotide; PCNA, proliferating cell nuclear marker; WISH, whole in situ hybridization.

produces erythrocytes and some primitive macrophages, and definitive hemopoiesis, which gives rise to long-term hemopoietic stem cells (HSCs) capable of unlimited self-renewal that generate all mature hemopoietic lineages (19). In zebrafish, primitive hemopoiesis occurs in the intermediate cell mass (ICM) located in the trunk and in the rostral blood island, whereas definitive hemopoiesis occurs in the dorsal aorta-posterior cardinal vein (DA-PCV) joint region, which is equivalent to the mammal aorta-gonad-mesonephros (AGM) region (18). Recently, an intermediate site of hemopoiesis, the caudal hemopoietic tissue (CHT) has been described (20). This site represents a transitional niche whose function would resemble that of the mammalian fetal liver.

In the present study we have investigated the role of PGE$_2$/EP4 signaling in thymus development in vivo. We show *ep4a* expression in the thymus rudiment by 48 hpf and in the AGM, where definitive hemopoiesis arises, by 26 hpf. Additionally, we show that PGE$_2$, via the EP4 receptor, increases the expression of the T cell precursor marker *rag1* within the thymus. Moreover, embryos lacking EP4 show a strong reduction of *rag1* in the thymus as well as that of *ikaros*-expressing cells in definitive hemopoietic tissues. These results seem to indicate that the PGE$_2$/EP4 pathway could be involved in the lymphoid cell fate decision.

Materials and Methods

Zebrafish colony

Zebrafish were bred and maintained as described (21). *Cloche* mutants and *fli1*::*GFP* transgenic line were provided by Drs. M. Schorpp (Max-Planck Institute of Immunobiology, Freiburg, Germany) and F. Cotelli (University of Milan, Milan, Italy), respectively.

ep2, ep4a, *and* ep4b *cDNA cloning*

By using the human EP-4 protein (GenBank accession no. AAA36434; previously misnamed EP2; Ref. 22) as a query, we searched the zebrafish expressed sequence tag database and identified three complete cDNA clones (National Center for Biotechnology Information accession nos. DQ286580, XM685848, and DQ202321). The protein sequences of these clones were aligned and showed high similarity to that of the mammalian PGE$_2$ receptor EP4 (DQ202321 and XM685848) and EP2 (DQ286580). Homology search was conducted using the Basic Local Alignment Search Tool (BLAST) (23). EP4a (DQ202321) and EP2 (DQ286580) have previously been described (24).

In situ hybridization, RT-PCR analysis and morpholinos

Whole-mount in situ hybridization was performed as described (25). Analysis of the expression of *ep4a* by RT-PCR was performed using total RNA from the developmental stages 24 hpf, 48 hpf, 3 days postfertilization (dpf), and 4 dpf and from ovaries extracted from adult fish. RT-PCR was conducted using the following primers: 5′-TGCTCAATCCCGCTTGTTGTC C-3′ (zEP4a-SGF1) and 5′-CGAAGCGGATGGCCAGAAGAT-3′ (zEP4a-SGR1); 5′-ATCGTTCTCATAGCCACGTCCACT-3′ (zEP4b-SGF1) and 5′-CCGGGTTTGGTCTTGCTGATGAAT-3′ (zEP4b-SGR1); and 5′-GGTGCT GCTGTGGTTCATGACAAT-3′ (zEP2-SGF1) and 5′-TGTTTCTGTGACG ATCTCGGTGGT-3′ (zEP2-SGR1). Morpholino oligonucleotides (MOs) were purchased from Gene Tools. The following MOs were designed against the 5′-untranslated region (MO1) and the predicted start codon (MO2) of *ep4a* (underlining indicates the predicted start codon): 5′-GATCGCGCTAAGCA GGCATTTTATC-3′ (*ep4a*-MO1) and 5′-CACGGTGGGCTCCATGCTGC TGCTG-3′ (*ep4a*-MO2). The *ep4a*-MO2 sequence was designed as described (24). In our experiments, MOs were injected at doses that resulted in minimal morphological deformities (0.13 pmol/embryo).

MATLAB analysis

Brightfield images of zebrafish embryos stained for *rag1* mRNA by whole in situ hybridization (WISH) were photographically inverted to compare the signal intensity between different treatments. Several random WISH images per treatment were selected, the positive thymus signal was centered, and images were rescaled to 200 × 261 pixels and imported into MATLAB software as a two-dimensional matrix representing pixel intensity. A three-dimensional array was created by concatenating individual images in the *Z* dimension. From this array, the mean value of pixel intensity in the *Z* dimension was calculated for each pixel, resulting in a two-dimensional matrix (26).

Immunohistochemestry

Dechorionated zebrafish embryos were collected and fixed overnight at 4°C in a solution of 4% paraformaldehyde in PBS containing 1% Tween 20 (PBT solution). Embryos were permeabilized by proteinase K treatment (25 μg/ml) for 1 h and then fixed. Samples were washed in PBT solution and blocked with 10% sheep serum at room temperature. Primary and secondary Abs were added overnight at 4°C in PBT solution. Ab dilution was 1/200 (Alexa Fluor 488 and mouse anti-proliferating cell nuclear Ag (PCNA); Santa Cruz Biotechnology).

Pharmacological experiments

Commercially available PGE$_2$ and PGD$_2$, COX2-inh (NS-398), COX1-inh (SC-560), and indomethacin (COX1/2-inh) were from Cayman Chemical. The selective COX2-inh SC-236 was provided by Drs. G. Folco and C. Buccellati, University of Milan, Milan, Italy. Butaprost and AH23848 were from Sigma-Aldrich. We supplemented wild-type embryos with 50 μM PGE$_2$, 10–50 μM PGD$_2$, 10 μM AH23848, and 25–50 μM of COX inh.

Statistics

Statistical significance ($p < 0.05$) was determined by the two-tailed Student *t* test.

Results

Ep4a *is expressed by hemopoietic/lymphoid tissues during embryonic zebrafish development*

Recently two orthologues of the human PGE$_2$ receptors EP2 and EP4 have been described in zebrafish (24). We sought to identify the entire repertoire of zebrafish EP receptors to examine their expression and role in thymus development. By using the tBLASTn search algorithm of the National Center for Biotechnology Information we obtained a sequence orthologous to human *ep2* and two sequences orthologous to human *ep4* named *ep4a* and *ep4b*. Zebrafish *ep1* and *ep3* orthologues were not found. We detected *ep2* and *ep4a* transcripts by RT-PCR at 24 hpf and up to 4 dpf, whereas *ep4b* became undetectable at 48 hpf and re-expressed at 4 dpf (data not shown). This differential expression pattern suggests nonredundant functions between these two *ep4* isoforms.

We then investigated whether these genes were expressed in the thymus rudiment during zebrafish development by WISH. At 48 hpf *ep4a* was expressed in a bilateral anatomic structure where at later stages the thymus anlage appears (Fig. 1, *a–c*). In contrast, the other EP receptors were not detected in this position (data not shown). The earliest known thymus markers, namely *ikaros* and *foxn1*, begin to be expressed at 3 dpf (12, 15, 16). Therefore, we analyzed *ep4a* expression at this stage and later on. At 3.5, 4, and 5 dpf *ep4a* expression was maintained in the presumptive thymus anlage (Fig. 1, *d–f*). To better define whether *ep4a* was expressed within the thymus, we performed double WISH analysis at the 5-dpf stage using the T cell precursor markers *rag1* and *ep4a*. The double labeling showed a colocalization of both mRNAs in the thymus area, thus indicating that *ep4a* was indeed expressed in the thymus (Fig. 1*e*, purple staining, black arrowheads). Because the thymus is composed of an epithelial compartment and immigrant lymphoid progenitors that start to colonize the thymic rudiment by 65 hpf (27, 28), we sought to distinguish whether *ep4a* was expressed in one or both thymic cellular components. To address this issue, we took advantage of the *cloche* mutant line, which is devoid of endothelial cells, thus lacking T cell precursors within the thymus (29). WISH analysis showed that *ep4a* expression in the thymus of these mutants was considerably weaker than in wild-type embryos although not absent (Fig. 1*f*), demonstrating that *ep4a* was expressed in both thymic cellular components. Because it has been proposed that lymphoid precursors seeding the thymus arise from the AGM

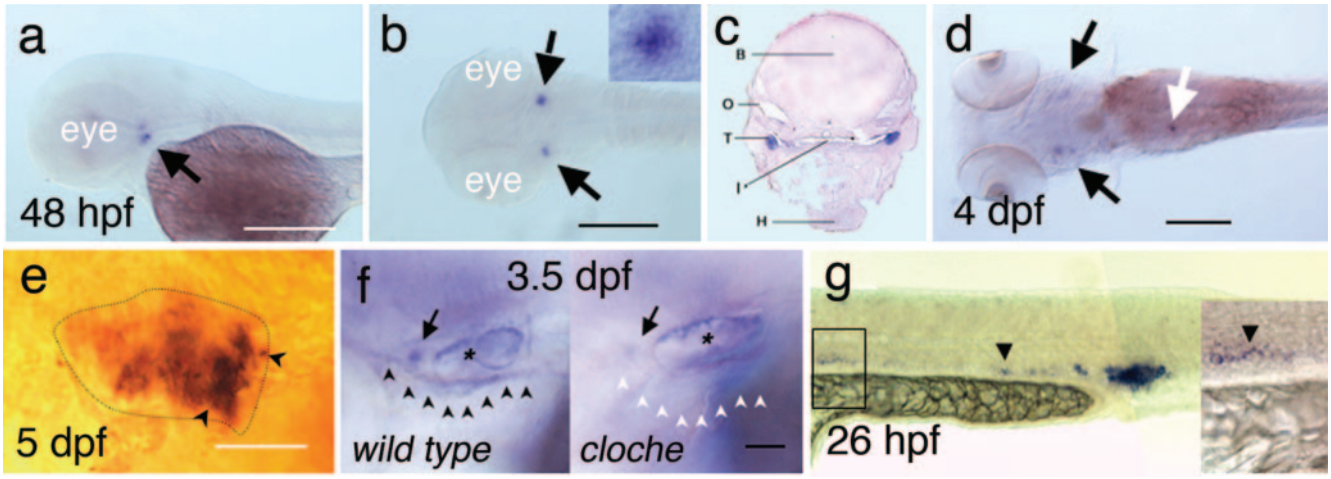

FIGURE 1. *ep4a* expression pattern in zebrafish embryos. WISH analyses for *ep4a* in zebrafish embryos at 26 hpf (*g*), 48 hpf (*a–c*), 3.5 dpf (*f*), 4 dpf (*d*), and 5 dpf (*e*). *a* and *b*, At 48 hpf *ep4a* is expressed only in the presumptive thymus rudiment (black arrows). *b*, Dorsal view showing bilateral *ep4a* expression in the presumptive thymus rudiment. *Inset*, A ×20 magnification of the thymus rudiment. *c*, Transverse section revealing the presumptive thymus rudiment location at an early stage of zebrafish development. *d*, Dorsal view. At 4 dpf *Ep4a* expression is maintained in the thymus rudiment (black arrows) and begins to be expressed where the liver appears (white arrow). *e*, Magnification of the thymus showing a double in situ hybridization analysis for *rag1* (red) and *ep4a* (blue). Black arrowheads indicate some cells expressing *ep4a* within the thymus delineated by *rag1* expression. *f*, Lateral views of wild-type and *cloche* mutant embryos at 3.5 dpf. *Ep4a* expression in the thymus rudiment (black arrow), blood vessels (black and white arrowheads), and ear (asterisks) of *wild type* and *cloche* embryos is shown. *Ep4a* expression in blood vessels is supported by the absence of *ep4a* expression in the *cloche* mutant (white arrowheads). The level of *ep4a* expression in the ear (asterisks) of the mutant represents an internal control of the staining. *g*, Lateral view of the trunk at 26 hpf showing *ep4a* expression in the AGM (black arrowheads). The *inset* is a magnification of the box in the figure. Scale bars, 200 μm (*a*, *b*, *d*, and *g*), 80 μm (*e*), and 35 μm (*f*). B, Brain; O, otic vesicle; T, thymus rudiment; I, pharynx; H, heart.

HSCs (19), we looked for *ep4a* expression in this site. By 26 hpf *ep4a* was detected in the AGM (Fig. 1*g*) with an expression pattern resembling that reported for c-*myb* (16). In contrast, *ep2* and *ep4b* were not detected (data not shown).

Taken together, these data indicate that *ep4a* is the earliest thymus marker identified to date. The expression of *ep4a* in sites of hemopoiesis (i.e., AGM) suggests a role for *ep4a* in T cell development.

PGE_2 treatment acting via EP4a increases rag1 *expression in the thymus*

PGE_2 is the naturally produced ligand of EP receptors. Moreover, it has been shown that zebrafish embryos produce PGE_2 during development (30). To investigate the role of PGE_2/EP4 signaling in the thymus and/or T cell development, we treated zebrafish embryos at 3 dpf when T cell precursors start to colonize the thymus, with PGE_2. Embryos were fixed after 24 h of incubation and the T cell precursor marker *rag1* was visualized by WISH. Thymi of PGE_2-treated embryos showed a stronger *rag1* expression than either control or DMSO-treated embryos (Fig. 2, *a* and *c*). To provide objective criteria and statistical backing to these differences of expression, we randomly took several images of the thymus of untreated ($n = 7$), DMSO-treated ($n = 7$), and PGE_2-treated ($n = 8$) embryos. After alignment of the thymus images, the mean pixel intensity was obtained by using the MATLAB software. This analysis showed an increase of the area highly expressing the *rag1* transcript in PGE_2-treated embryos compared with untreated or DMSO-treated embryos (Fig. 2*a*, *middle column*). Three-dimensional analysis confirmed an increase of pixel intensity in the *rag1*-treated thymus (Fig. 2*a*, *right column*). The increase of intensity between controls and PGE_2-treated embryos was statistically significant (Fig. 2*b*; **, $p < 0.005$). In contrast, the 24-h treatment with either COX1-inh (SC-560) or COX2-inh (SC-236), which blocks the endogenous PGE_2 synthesis, did not allow *rag1* expression in the thymus (Fig. 2*c*). In agreement with these results, images from thymi treated with the COX2-inh ($n = 4$) resulted in flat, three-dimensional pseudocolor graphs indicating levels of expression similar to background (Fig. 2*a*, *middle* and *right columns*). Again, the decrease of *rag1* expression was statistically significant (Fig. 2*b*, **, $p < 0.005$).

To simplify and extend the analysis to a larger number of embryos, we set up a quantitative WISH assay. Embryos were placed into three arbitrary categories (low/null, normal, and high; Fig. 3) depending on the level of *rag1* expression in the thymus. In different experiments, untreated embryos showed some variability in the expression of a given phenotype (normal, range 35.7–51.7%; null/low, range 14.7–38%; and high, range 25–44%). Therefore, the results were normalized by reporting in Table I the ratio of the percentage of embryos detected in treated and untreated embryos for each category. The quantitative WISH analysis confirmed the results obtained by using the MATLAB software. As reported in Table I, embryos treated with PGE_2 for 24 h showed a 1.8-fold increase of the high *rag1* phenotype (treated to untreated ratio was 46.2/26.5%), while the number of embryos with null/low phenotype decreased (treated to untreated ratio was 15.3/21.9%). The treatment with either COX inhibitor resulted in a complete null/low phenotype due to the whole lack of *rag1* signal in the thymus. Similar results were obtained using different COX inhibitors (NS-398 and indomethacin; data not shown). In addition, the response to COX2-inh was dose dependent (Table I). No such modifications were observed in DMSO-treated embryos. Furthermore, incubation of zebrafish embryos with other prostaglandins like PGD_2 did not influence *rag1* expression (Table I), indicating that the increase of *rag1* expression was PGE_2-dependent.

The role of PGE_2 was further supported by rescue experiments. As shown in Table I, PGE_2 was able to revert the phenotype elicited by COX2-inh, inducing a decrease of the null/low phenotype from 4.6 to 2.5 (treated to untreated ratio from 100/21.8% to 54/

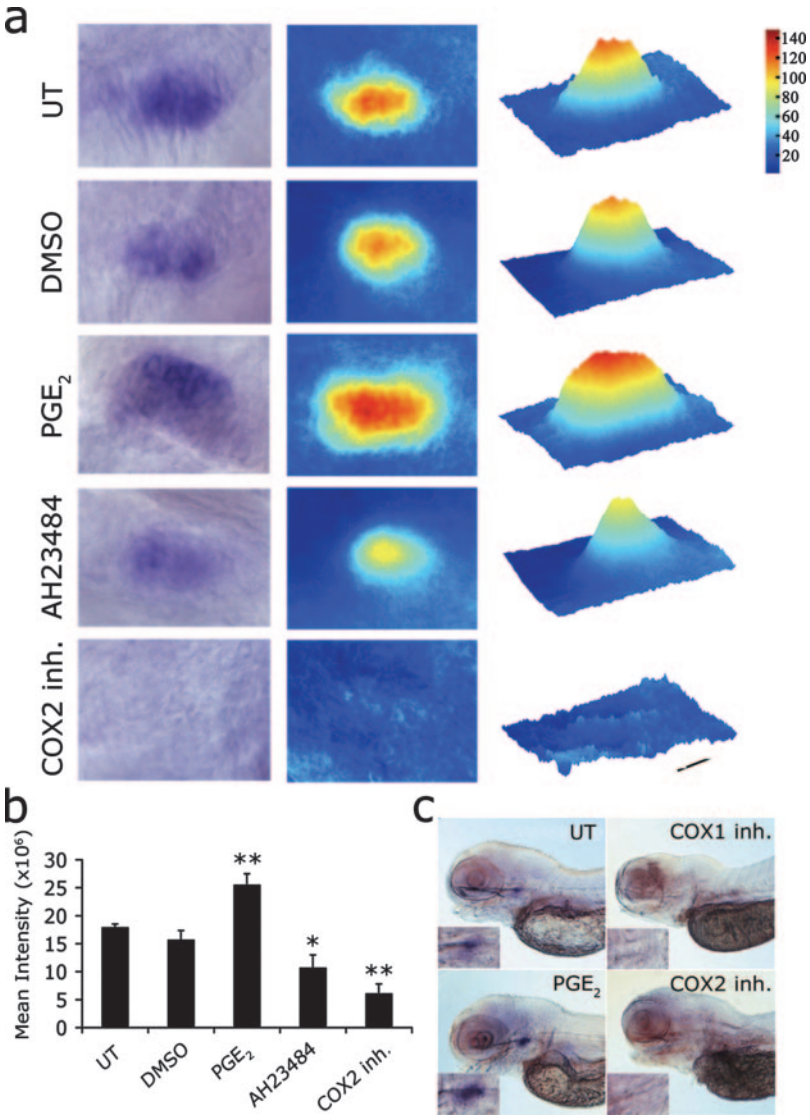

FIGURE 2. PGE$_2$, COX2-inh, and the EP4 antagonist AH23848 differentially affect *rag1* expression in the thymus of zebrafish embryos. *a*, Pseudocolor surface plots of the mean signal intensity (scale, 0–140) for *rag1* mRNA in the thymi of untreated (UT; $n = 7$) and DMSO- ($n = 7$), PGE$_2$- ($n = 8$), AH23848- ($n = 8$), and COX2-inh-treated ($n = 4$) embryos. The *left column* shows a representative WISH image of the thymus, the *middle column* represents the pseudocolor surface plot of the mean signal intensity obtained by concatenating individual images in the *Z* dimension, and the *right column* is a three-dimensional array showing the mean signal intensity in the *Z* axis. After PGE$_2$ exposure the area highly expressing *rag1* (red) is increased. In contrast, the intensity is reduced after the treatment with AH23848 (EP4 antagonist) and is completely absent following the incubation with COX2-inh. *b*, Graph representing the mean intensity of the *rag1* signal collected from control or treated embryos. *Rag1* expression in the thymus was increased by PGE$_2$ and reduced by treatments with AH23484 and COX2-inh. Asterisks indicate a statistically significant difference between treated embryos and controls (untreated (UT) and DMSO-treated embryos) based on Student's *t* test. *, $p < 0.05$; **, $p < 0.005$. *c*, Representative WISH images showing *rag1* expression in the thymus of control (UT) and treated embryos. Embryos were treated with PGE$_2$, COX1/2-inh, or COX2-inh for 24 h. PGE$_2$-treated embryos show an increase in the *rag1* signal, whereas COX1/2- or COX2-inh treated embryos show a complete inhibition of *rag1* expression. Each *inset* is a magnification of the thymus.

21.8%) and a partial increase of the high category from 0 to 0.2 (treated to untreated ratio from 0/26.5% to 6.25/26.5%). More importantly, we observed a rescue of the normal phenotype, which went from 0% for COX2-inh alone (treated to untreated ratio

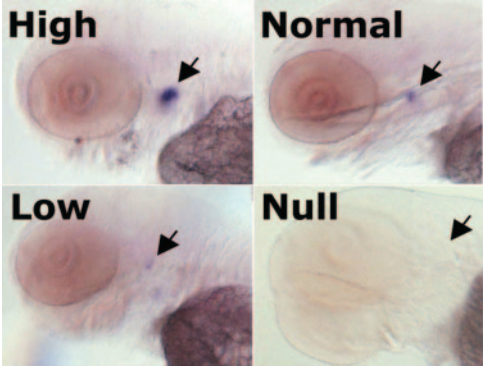

FIGURE 3. Arbitrary categories of *rag1* expression in thymi. Representative WISH images showing the different levels of *rag1* expression detected in untreated embryos. The three arbitrary categories null/low, normal, and high were defined according to the different levels of *rag1* expression in the thymus.

Table I. *WISH analysis of rag1 expression in the thymus of treated embryos*

Treatment[a]	*rag1* Expression (T/UT)[b]		
	Null/Low	Normal	High
PGE$_2$ ($n = 119$)	0.5	0.9	1.8
COX1/2-inh ($n = 50$)	4.6	0	0
COX2-inh (25 μM) ($n = 51$)	2.6	1.5	0
COX2-inh (50 μM) ($n = 51$)	4.6	0	0
COX1-inh plus PGE$_2$ ($n = 50$)	4.1	0.2	0
COX2-inh plus PGE$_2$ ($n = 49$)	2.5	0.8	0.2
PGD$_2$ ($n = 21$)	0.8	1.2	1.0
AH23848 ($n = 42$)	1.9	0.6	0.2
DMSO ($n = 70$)	1.0	1.0	1.0
EP4-MO1 ($n = 102$)	2.8	0.7	0.2
EP4-MO2 ($n = 74$)	4.3	0.9	0.5
Ctrl-MOs ($n = 75$)	1.2	1.3	0.4

[a] Embryos were injected with morpholino at 1-cell stage, or treated with the different compounds at 3 dpf. *Rag1* expression was analyzed at 4 dpf. *n*, Number of treated embryos.

[b] The level of *rag1* expression was scored as null/low, normal, or high in accordance with Fig. 3. The results were normalized by reporting the ratio of the percentages of positive embryos detected in treated (T) and in untreated (UT) animals for each category.

0/51.6% = 0 in Table I) to 41.6% by adding PGE_2 (treated to untreated ratio 41.6/51.6% = 0.8 in Table I), almost reaching the level detected in untreated embryos. On the contrary, the activity of COX1-inh was only slightly affected by the PGE_2 addition (Table I). Thus, a direct role of the COX2/PGE_2 pathway in regulating *rag1* expression in the thymus is demonstrated.

Because EP4 was the only PGE_2 receptor detected in the thymus, we sought to verify whether PGE_2 activity was indeed exerted via the EP4 receptor. To address this question we used the EP2 agonist butaprost and the EP4-specific antagonist AH23848. Butaprost treatment for 24 h did not increase *rag1* expression, in accordance with the absence of *ep2* transcripts in the thymus (data not shown). In contrast, embryos treated with AH23848 showed a marked inhibition of *rag1* transcripts (Table I). The MATLAB analysis of thymi from embryos treated with the AH23848 ($n = 8$) demonstrated a statistically significant reduction of *rag1* expression compared with controls (Fig. 2, *a* and *b*, *, $p < 0.05$). To confirm this inhibition, we genetically blocked *ep4a* by performing MO knockdown experiments (31). Because the treatment with 0.26 pmol/embryo results in gastrulation defects (24), we tested lower concentrations to identify the dose (i.e., 0.13 pmol/embryo) allowing a normal gastrulation process. The injection of either *ep4a*-MO1 or *ep4a*-MO2 at 0.13 pmol/embryo caused an increase of 2.8- and 4.3-fold, respectively, of embryos with a null/low *rag1* expression category in comparison with untreated embryos (treated to untreated ratio was 70/39% and 26/6%, respectively). As expected, the control MOs did not increase this category (Table I).

To verify whether the absence of $rag1^+$ cells within the thymus upon EP4 inhibition was due to the induction of apoptosis, we performed TUNEL experiments. The thymi of 5 dpf embryos treated with PGE_2, AH23848, or left untreated showed a similar number of apoptotic cells (data not shown), demonstrating that the decrease of *rag1*-expressing cells in the thymus upon EP4 inhibition was not due to programmed cell death. Based on this we can conclude that the PGE_2/EP4 signaling in the thymus controls the expression of *rag1*.

PGE_2 induces cell proliferation in the zebrafish thymus

The *Rag1* signal in the thymi of PGE_2-treated embryos was more widespread than in control siblings (Figs. 2*a* and 3). This hybridization pattern suggests that the increase in *rag1* expression is not likely due to enhanced transcription in single cells. Therefore, we sought to ascertain whether the PGE_2-induced increase of *rag1* expression was due to either an enlargement of thymus, and therefore an increase in the total number of epithelial cells, or to an increased number of $rag1^+$ cells. Indeed, in vitro experiments have shown that PGE_2 protects human thymocytes from apoptosis (32) and induces thymocyte differentiation from DN to DP cells (7). We first tested whether the PGE_2/EP4 pathway was able to settle the thymus architecture. The epithelial component of the thymus did not undergo significant changes in size upon PGE_2 treatment as evaluated by using *foxn1,* a specific marker for the epithelial compartment of the zebrafish thymus (15) (Fig. 4, *a* and *b*). These results were further confirmed by treating embryos with either the EP4 antagonist AH23848 or the COX-inh or by injecting the EP4-MOs (Fig. 4, *c–f*). We then tested whether PGE_2 could favor T cell precursor differentiation by inducing *rag1* expression. To this end we provided PGE_2 to zebrafish embryos for 12 or 24 h at 48 hpf when *ep4a* but not *rag1* is expressed. No changes in *rag1* expression kinetics could be detected by WISH (data not shown), suggesting that PGE_2 was not favoring thymus differentiation by inducing the premature expression of *rag1*. We next investigated whether, upon PGE_2 exposure, the proliferation rate of T cell precursors was increased. By using the PCNA we observed that PGE_2-treated embryos showed $PCNA^+$ cells in the thymus (Fig. 4*h*), whereas the control and AH23848-treated embryos did not (Fig. 4, *g* and *i*). Taken together, these data indicate that PGE_2, acting via the EP4 receptor, increases the number of *rag1*-expressing cells as well as cell proliferation in the zebrafish thymus.

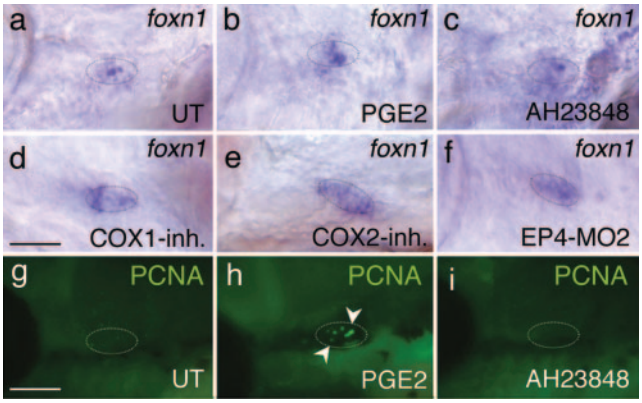

FIGURE 4. PGE_2 triggers cell proliferation within thymus anlage. *a–f*, Lateral view, 4 dpf. WISH analysis detected the thymic epithelial marker *foxn1* in the thymus rudiment of untreated (UT) (*a*) and PGE2- (*b*), AH23848- (*c*), COX1/2-inh- (*d*), and COX2-inh-treated (*e*) embryos or EP4-MO2-injected embryos (*f*). Dashed ovals show thymus location. No significant difference in *foxn1* expression is observed. *g–i*, Immunofluorescence analysis showing the proliferation marker PCNA at 4 dpf in untreated (UT) (*g*) and PGE_2- (*h*) and AH23848-treated (*i*) embryos. White dashed ovals indicate thymus border. The treatment with PGE_2 induces the selective accumulation of $PCNA^+$ cells within the thymus (*h*, white arrowheads). Scale bar, 75 μm.

Blocking PGE_2/EP4 signaling interferes with early lymphoid precursor development

We detected *ep4a* expression at 26 hpf in the AGM, where definitive hemopoiesis arises (Fig. 1*g*). Therefore, we hypothesized that, in EP4-lacking embryos, the absence of *rag1*-expressing cells in the thymus could be due to the impairment of T cell progenitor differentiation in hemopoietic sites. The origin of the lymphoid progenitors that seed the zebrafish thymus is unknown. However, a population of $ikaros^+$ cells present in the ventral wall of the dorsal aorta is thought to be the most likely source (16). At 24 hpf *ikaros*-expressing cells can be detected in the DA-PCV joint region. At 48 hpf those cells can be detected throughout the pharyngeal arches and later they can be detected in the thymus (16).

To investigate the role of the PGE_2/EP4 pathway in controlling $ikaros^+$ cell differentiation, we injected embryos with either *ep4a*-MO1 or *ep4a*-MO2. This led to a marked and statistically significant reduction of the expression of *ikaros* in the AGM at 24 hpf (Fig. 5, *a* and *b*, and data not shown). At 5 dpf we observed a strong reduction of the expression of *ikaros* in *ep4a*-MO2-injected embryos in a region resembling the recently described CHT (Fig. 5, *f* and *g*; arrowheads). Accordingly, the addition of either the EP4 antagonist (i.e., AH23848) or PGE_2 partially reduced or modestly increased the level of *ikaros* expression in the AGM (Fig. 5, *c–e*). The absence of $ikaros^+$ HSCs in the AGM and the CHT upon inhibition of the PGE_2/EP4 pathway was not due to apoptotic cell death as evaluated by TUNEL experiments (data not shown). These results demonstrate that the PGE_2/EP4 pathway acts upstream of the differentiation of $rag1^+$ cells, affecting the differentiation of *ikaros*-expressing cells in the AGM and in the CHT.

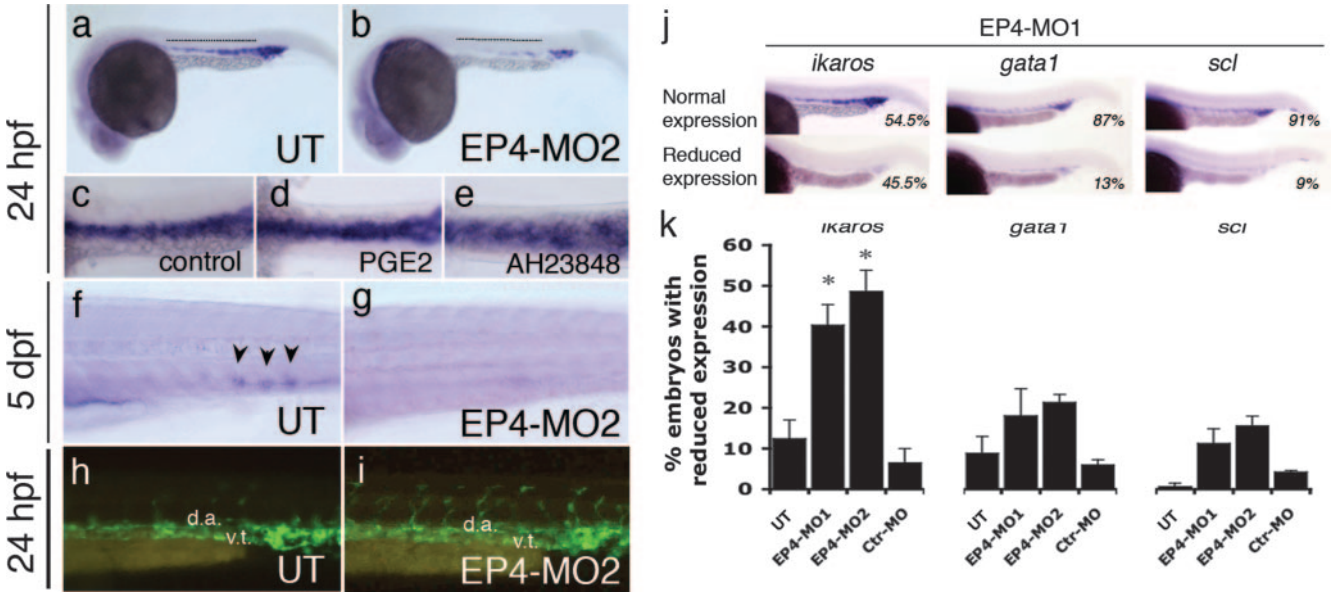

FIGURE 5. PGE$_2$/EP4 signaling controls the expression of *ikaros* in definitive hemopoietic tissues without affecting vasculogenesis and myeloerythroid fate decision. *a* and *b*, Lateral views at 24 hpf. WISH analyses were performed using the T cell progenitor marker *ikaros*. EP4-MO2-injected embryos show a strong decrease of *ikaros* expression in the AGM (*b*) compared with control untreated (UT) embryos (*a*). Dashed line indicates the AGM. *c–e*, Ventral views at 24 hpf. Magnification of the areas highlighted by the dashed lines in *a* and *b* showing a ventral view of the region above the yolk sac (anterior left; posterior right) of untreated (*c*) and PGE$_2$- (*d*) and AH23848-treated (*e*) embryos. *f* and *g*, Lateral views at 5 dpf. Untreated embryos showing *ikaros* expression in the caudal hemopoietic tissue (CHT) (*f*, black arrowheads). *Ep4a*-MO2-injected embryos (*g*) do not express *ikaros* in the CHT. *h* and *i*, *fli1*::*GFP* transgenic lines that express GFP in developing blood vessels were injected with *ep4a*-MO1. Both control embryos (*h*) as well as *ep4a*-MO1-injected embryos (*i*) show normal blood vessel development. d.a, Dorsal aorta; v.t., vascular tube. *j*, Representative WISH images from one experiment showing normal and reduced expression of *ikaros*, *gata1*, and *scl* in the ICM of EP4-MO1-injected embryos. Percentages of normal and reduced expression are reported. *k*, Graphs showing the results obtained from three independent experiments. EP4-MO1- and EP4-MO2-injected embryos showed a significant reduction in *ikaros* expression ($p < 0.005$; $n = 96$), whereas *gata1* and *scl* were not significantly affected. UT, Untreated.

To investigate whether ep4a could interfere with the development of the vascular tube and dorsal aorta, we took advantage of the *fli1*::*GFP* transgenic line (33) whose blood vessels constitutively express GFP. The expression of GFP was intact in embryos treated with PGE$_2$, AH23848, or EP4-MO1 both at 24 hpf and 5 dpf (Fig. 5, *h* and *i*, and data not shown). Furthermore, the analysis of vessel and artery formation by using WISH for *flk-1* and *ephrinB2*, respectively, did not show any difference between control and EP4-lacking embryos (data not shown). Thus, we demonstrate that the absence of *ikaros*$^+$ cells mediated by EP4 inhibition was not due to defects in vascular tube or dorsal aorta specification.

To confirm the specific role of the PGE$_2$/EP4 pathway in lymphoid cell differentiation, we analyzed the expression of the HSC markers *scl*, *gata1*, and *gata2* at 24 hpf following the injection with *ep4a*-MO1, *ep4a*-MO2, or MOs control. An example of the expression patterns (i.e., normal and reduced) observed upon the treatments (e.g., *ep4a*-MO1) is reported in Fig. 5*j*. The expression of *scl*, *gata1*, and *gata2* in the ICM of either *ep4a*-MO1- or *ep4a*-MO2-injected embryos was not significantly altered, whereas a statistically significant reduction of *ikaros* expression was observed (Fig. 5*k* and data not shown). Thus, the involvement of *ep4a* in lymphoid precursors development is indicated.

In conclusion, these results indicate that the PGE$_2$/EP4 pathway acts downstream of the activation of *gata2* in the differentiation of a nonerythropoietic, lymphoid-specific (*ikaros*$^+$) precursor.

Discussion

In this report, we demonstrate that the PGE$_2$/EP4 pathway is involved in lymphoid precursor development in zebrafish. Indeed, the inhibition of PGE$_2$ production abrogated *rag1* expression within the thymus, whereas its addition induced an increase of *rag1*-expressing cells. Importantly, we demonstrate pharmacologically and genetically that *rag1* induction occurs specifically via the EP4 receptor. Interestingly, we find another *ep4* isoform (i.e., *ep4b*) that is not expressed in the AGM or the thymus (data not shown), which suggests different roles for the two EP4 isoforms.

In zebrafish, the thymic anlage is first detectable by 60 hpf by ultrastructural analysis (18). At this time, T cell precursors begin to seed the thymus (13, 28). *ikaros* is the first lymphoid-related gene detected in the thymus (16, 34) at 72 hpf. Later on (92 hpf), developing thymocytes begin to express *rag1* and *rag2* (27, 34). Interestingly, by 48 hpf we found that *ep4a* was expressed bilaterally in the presumptive thymus rudiment. Later, the expression was maintained and colocalized with *rag1*, demonstrating that *ep4a* was indeed expressed in the thymus. Thus, to our knowledge *ep4a* becomes the earliest thymus marker described to date, useful for tracking thymus development in zebrafish.

By using the *cloche* mutant lacking the entire hemopoietic cell lineage (29), we demonstrated that *ep4a* was expressed in both the thymic epithelium as well as in T cell precursors, a finding consistent with previous in vitro studies in mammals (5, 6). The idea that *ep4a* is expressed by T cell precursors was supported by the strong reduction of *ep4a* expression observed in the *cloche* mutant as well as by the detection of *ep4a* expression in the DA-PCV joint region, where definitive hemopoiesis arises. Further studies will be needed to clarify the role of *ep4a* in the epithelial cells of the thymus.

In agreement with these findings, pharmacological and genetic inhibition of EP4 reduced *rag1* expression in the thymus without evidence of cell death, whereas the treatment of embryos with PGE_2 induced cell proliferation in the thymus (Fig. 4*h*). Whether proliferating cells belong to the thymic epithelium, the T cell lineage or both remains unclear. The fact that the inhibition of EP4 induced a partial reduction of *rag1* while we observed a complete reduction in embryos incubated with COX-inh could be due to the lower doses of EP4-MOs (0.13 pmol/embryo) used to preserve the gastrulation process (24). Alternatively, we may hypothesize a role for other PG derivatives in T cell development. In an in vitro murine model it has been shown that the effect of the COX2-inh NS-398 in T cell development is COX2- and PGE_2-independent; indeed, PGE_2 was not able to reverse the effect of NS-398 in fetal thymic organ culture (8). In our system the effect of COX1-inh was poorly reversed while that of COX2 was rescued by PGE_2, suggesting that the COX1-inh could act in a PGE_2-independent manner while the effect of COX2-inh was mainly due to the inhibition of PGE_2. However, we cannot exclude the possibility that the activity of COX1-inh, used at lower concentration, could be reverted by PGE_2.

Moreover, a pharmacological and genetic blockade of the EP4 receptor recapitulated the inhibition of *rag1* seen with COX2-inh, further confirming a PGE_2-dependent mechanism in the regulation of *rag1*-expressing cells in the thymus.

In this study, we consistently found *ep4a* expression in the DA-PCV joint region at 26 hpf (Fig. 1*g*), where definitive hemopoiesis arises. Inhibition of EP4 abolished the expression of the lymphoid precursor marker *ikaros* in the AGM and at 5 dpf in the CHT. Additional experiments using transgenic fluorescent reporter lines and/or cell transplants will elucidate the direct lineage relationship between *ikaros*-expressing cells in the DA-PCV joint region and CHT and the *rag1*-expressing cells in the thymus. The inhibition of *ikaros* expression mediated by EP4 blockade indicates that the PGE_2/EP4 pathway might play a novel role in hemopoiesis, specifically in lymphopoiesis. This hypothesis was confirmed by dissecting the role of the PGE_2/EP4 pathway at different steps of hemopoietic specification. *scl* and *gata2* are genes encoding essential transcription factors for vertebrate hemopoietic specification (19). In zebrafish, the ablation of *scl* results in loss of primitive and definitive hemopoiesis (35). In contrast, GATA1-null mice and GATA1-lacking cell lines have defective erythroid gene expression (36, 37). Moreover, in zebrafish embryos it has been shown that *gata1* regulates the myeloerythroid fate decision (38). Our results demonstrate that loss of *ep4a* does not significantly affect the expression of *scl* and *gata2*, which are located upstream of *ikaros*, as well as the expression of the erythroid progenitor marker *gata1* (Fig. 4, *h* and *i*, and data not shown), thus confirming that EP4 is dispensable for the early steps of HSC specification.

Although PGE_2 signaling has been shown to promote thymocyte differentiation and protection from apoptosis (7, 32), its role and the mechanism by which it is involved in T cell development in vivo are completely unknown. Differing from our results in morpholino knockout embryos, studies performed in COX1/2 double-knockout mice have shown that PGE_2 seems to play a marginal role in T cell development (8). However, in both systems stronger effects were observed when chemical inhibitors were used. These observations suggest a greater PGE_2 dependence for T cell development in mammals than in zebrafish, perhaps because of a lower level of redundancy; alternatively, it may reflect on the difference of the experimental systems used (i.e., the in vivo model for zebrafish or the ex vivo model for the murine fetal thymic organ cultures).

Our studies provide the first evidence that PGE_2 signaling through the EP4 receptor regulates lymphocyte precursors homeostasis in vivo. Understanding the detailed mechanism of PGE_2 signaling in zebrafish T cell development may provide significant insights into how PGE_2 regulates the immune response in mammals and how it may influence the onset of immune system diseases such as autoimmunity or hemological malignancies. In contrast, this study suggests that the expansion/differentiation of $rag1^+$ cells in the thymus could be a mechanism used to generate mature T cells during inflammation, a process associated with the production of relevant amounts of PGE_2.

Acknowledgments

We thank Michael Schorpp and Cristián Soza Ried for providing us with the *cloche* mutant. We are grateful to Anna Mondino for critically reading the manuscript.

Disclosures

The authors have no financial conflict of interest.

References

1. Hata, A. N., and R. M. Breyer. 2004. Pharmacology and signaling of prostaglandin receptors: multiple roles in inflammation and immune modulation. *Pharmacol. Ther.* 103: 147–166.
2. Park, J. Y., M. H. Pillinger, and S. B. Abramson. 2006. Prostaglandin E_2 synthesis and secretion: the role of PGE_2 synthases. *Clin. Immunol.* 119: 229–240.
3. Narumiya, S. 2003. Prostanoids in immunity: roles revealed by mice deficient in their receptors. *Life Sci.* 74: 391–395.
4. Harizi, H., and N. Gualde. 2005. The impact of eicosanoids on the crosstalk between innate and adaptive immunity: the key roles of dendritic cells. *Tissue Antigens* 65: 507–514.
5. Ushikubi, F., M. Hirata, and S. Narumiya. 1995. Molecular biology of prostanoid receptors; an overview. *J. Lipid Mediators Cell Signal.* 12: 343–359.
6. Appasamy, P. M., K. Pendino, R. R. Schmidt, K. P. Chepenik, M. B. Prystowsky, and D. Goldowitz. 1991. Expression of prostaglandin G/H synthase (cyclooxygenase) during murine fetal thymic development. *Cell. Immunol.* 137: 341–357.
7. Rocca, B., L. M. Spain, E. Pure, R. Langenbach, C. Patrono, and G. A. FitzGerald. 1999. Distinct roles of prostaglandin H synthases 1 and 2 in T-cell development. *J. Clin. Invest.* 103: 1469–1477.
8. Xu, H., D. J. Izon, C. Loftin, and L. M. Spain. 2001. The COX-2 inhibitor NS-398 causes T-cell developmental disruptions independent of COX-2 enzyme inhibition. *Cell. Immunol.* 214: 184–193.
9. Goetzl, E. J., S. An, and L. Zeng. 1995. Specific suppression by prostaglandin E_2 of activation-induced apoptosis of human $CD4^+CD8^+$ T lymphoblasts. *J. Immunol.* 154: 1041–1047.
10. Trede, N. S., A. Zapata, and L. I. Zon. 2001. Fishing for lymphoid genes. *Trends Immunol.* 22: 302–307.
11. Boehm, T., C. C. Bleul, and M. Schorpp. 2003. Genetic dissection of thymus development in mouse and zebrafish. *Immunol. Rev.* 195: 15–27.
12. Trede, N. S., D. M. Langenau, D. Traver, A. T. Look, and L. I. Zon. 2004. The use of zebrafish to understand immunity. *Immunity* 20: 367–379.
13. Langenau, D. M., and L. I. Zon. 2005. The zebrafish: a new model of T-cell and thymic development. *Nat. Rev. Immunol.* 5: 307–317.
14. Cha, Y. I., L. Solnica-Krezel, and R. N. DuBois. 2006. Fishing for prostanoids: deciphering the developmental functions of cyclooxygenase-derived prostaglandins. *Dev. Biol.* 289: 263–272.
15. Schorpp, M., M. Leicht, E. Nold, M. Hammerschmidt, A. Haas-Assenbaum, W. Wiest, and T. Boehm. 2002. A zebrafish orthologue (whnb) of the mouse nude gene is expressed in the epithelial compartment of the embryonic thymic rudiment. *Mech. Dev.* 118: 179–185.
16. Willett, C. E., H. Kawasaki, C. T. Amemiya, S. Lin, and L. A. Steiner. 2001. Ikaros expression as a marker for lymphoid progenitors during zebrafish development. *Dev. Dyn.* 222: 694–698.
17. Bhandoola, A., and A. Sambandam. 2006. From stem cell to T cell: one route or many? *Nat. Rev. Immunol.* 6: 117–126.
18. Davidson, A. J., and L. I. Zon. 2004. The 'definitive' (and 'primitive') guide to zebrafish hematopoiesis. *Oncogene* 23: 7233–7246.
19. de Jong, J. L., and L. I. Zon. 2005. Use of the zebrafish system to study primitive and definitive hematopoiesis. *Annu. Rev. Genet.* 39: 481–501.
20. Murayama, E., K. Kissa, A. Zapata, E. Mordelet, V. Briolat, H. F. Lin, R. I. Handin, and P. Herbomel. 2006. Tracing hematopoietic precursor migration to successive hematopoietic organs during zebrafish development. *Immunity* 25: 963–975.
21. Solnica-Krezel, L., A. F. Schier, and W. Driever. 1994. Efficient recovery of ENU-induced mutations from the zebrafish germline. *Genetics* 136: 1401–1420.
22. Bastien, L., N. Sawyer, R. Grygorczyk, K. M. Metters, and M. Adam. 1994. Cloning, functional expression, and characterization of the human prostaglandin E_2 receptor EP2 subtype. *J. Biol. Chem.* 269: 11873–11877.
23. Altschul, S. F., W. Gish, W. Miller, E. W. Myers, and D. J. Lipman. 1990. Basic local alignment search tool. *J. Mol. Biol.* 215: 403–410.

24. Cha, Y. I., S. H. Kim, D. Sepich, F. G. Buchanan, L. Solnica-Krezel, and R. N. DuBois. 2006. Cyclooxygenase-1-derived PGE_2 promotes cell motility via the G-protein-coupled EP4 receptor during vertebrate gastrulation. *Genes Dev.* 20: 77–86.
25. Jowett, T., and L. Lettice. 1994. Whole-mount in situ hybridizations on zebrafish embryos using a mixture of digoxigenin- and fluorescein-labelled probes. *Trends Genet.* 10: 73–74.
26. Court, F. A., D. L. Sherman, T. Pratt, E. M. Garry, R. R. Ribchester, D. F. Cottrell, S. M. Fleetwood-Walker, and P. J. Brophy. 2004. Restricted growth of Schwann cells lacking Cajal bands slows conduction in myelinated nerves. *Nature* 431: 191–195.
27. Willett, C. E., A. G. Zapata, N. Hopkins, and L. A. Steiner. 1997. Expression of zebrafish rag genes during early development identifies the thymus. *Dev. Biol.* 182: 331–341.
28. Willett, C. E., A. Cortes, A. Zuasti, and A. G. Zapata. 1999. Early hematopoiesis and developing lymphoid organs in the zebrafish. *Dev. Dyn.* 214: 323–336.
29. Parker, L., and D. Y. Stainier. 1999. Cell-autonomous and non-autonomous requirements for the zebrafish gene cloche in hematopoiesis. *Development* 126: 2643–2651.
30. Grosser, T., S. Yusuff, E. Cheskis, M. A. Pack, and G. A. FitzGerald. 2002. Developmental expression of functional cyclooxygenases in zebrafish. *Proc. Natl. Acad. Sci. USA* 99: 8418–8423.
31. Ekker, S. C., and J. D. Larson. 2001. Morphant technology in model developmental systems. *Genesis* 30: 89–93.
32. Pica, F., O. Franzese, C. D'Onofrio, E. Bonmassar, C. Favalli, and E. Garaci. 1996. Prostaglandin E_2 induces apoptosis in resting immature and mature human lymphocytes: a c-Myc-dependent and Bcl-2-independent associated pathway. *J. Pharmacol. Exp. Ther.* 277: 1793–1800.
33. Lawson, N. D., and B. M. Weinstein. 2002. In vivo imaging of embryonic vascular development using transgenic zebrafish. *Dev. Biol.* 248: 307–318.
34. Lam, S. H., H. L. Chua, Z. Gong, T. J. Lam, and Y. M. Sin. 2004. Development and maturation of the immune system in zebrafish, *Danio rerio*: a gene expression profiling, in situ hybridization and immunological study. *Dev. Comp. Immunol.* 28: 9–28.
35. Juarez, M. A., F. Su, S. Chun, M. J. Kiel, and S. E. Lyons. 2005. Distinct roles for SCL in erythroid specification and maturation in zebrafish. *J. Biol. Chem.* 280: 41636–41644.
36. Weiss, I. M., and S. A. Liebhaber. 1994. Erythroid cell-specific determinants of α-globin mRNA stability. *Mol. Cell. Biol.* 14: 8123–8132.
37. Pevny, L., C. S. Lin, V. D'Agati, M. C. Simon, S. H. Orkin, and F. Costantini. 1995. Development of hematopoietic cells lacking transcription factor GATA-1. *Development* 121: 163–172.
38. Galloway, J. L., R. A. Wingert, C. Thisse, B. Thisse, and L. I. Zon. 2005. Loss of gata1 but not gata2 converts erythropoiesis to myelopoiesis in zebrafish embryos. *Dev. Cell.* 8: 109–116.